Naval Research Laboratory

Washington, DC 20375-5320

NRL/MR/6180--07-9045

Heat Release Rates for Shipboard Dry Goods Storage Space Materials

JOHN B. HOOVER
HUNG PHAM
FREDERICK W. WILLIAMS

Navy Technology Center for Safety and Survivability
Chemistry Division

May 4, 2007

REPORT DOCUMENTATION PAGE

Form Approved
OMB No. 0704-0188

1. REPORT DATE *(DD-MM-YYYY)*	**2. REPORT TYPE**	**3. DATES COVERED** *(From - To)*
04-05-2007	Final Report	

4. TITLE AND SUBTITLE

Heat Release Rates for Shipboard Dry Goods Storage Space Materials

5a. CONTRACT NUMBER

5b. GRANT NUMBER

5c. PROGRAM ELEMENT NUMBER

6. AUTHOR(S)

John B. Hoover, Hung Pham, and Frederick W. Williams

5d. PROJECT NUMBER

5e. TASK NUMBER

5f. WORK UNIT NUMBER

7. PERFORMING ORGANIZATION NAME(S) AND ADDRESS(ES)

Naval Research Laboratory
4555 Overlook Avenue, SW
Washington, DC 20375-5320

8. PERFORMING ORGANIZATION REPORT NUMBER

NRL/MR/6180--07-9045

9. SPONSORING / MONITORING AGENCY NAME(S) AND ADDRESS(ES)

Office of the Secretary of Defense
Joint Live Fire Test & Evaluation
Washington, DC

10. SPONSOR / MONITOR'S ACRONYM(S)

11. SPONSOR / MONITOR'S REPORT NUMBER(S)

12. DISTRIBUTION / AVAILABILITY STATEMENT

Approved for public release; distribution is unlimited.

13. SUPPLEMENTARY NOTES

14. ABSTRACT

Compartment-scale tests were conducted to evaluate the fire performance of items found in typical dry goods storage spaces on DDG-51 class destroyers. Packaging materials included cardboard boxes, Kraft paper and polyethylene bubble wrap. Toilet paper, paper towels, and copy paper were used as representative flammable stock items. Heat release rate (HRR) was measured by oxygen consumption calorimetry. It was found that both the nature of the material and the packing density affected the peak HRR. Polyethylene produced higher values than paper materials due to the greater heat of combustion; low density packing led to higher HRR than high density packing, due to greater oxygen availability.

15. SUBJECT TERMS

Fire, Cardboard, Polyethylene, Storage space, Paper

16. SECURITY CLASSIFICATION OF:			**17. LIMITATION OF ABSTRACT**	**18. NUMBER OF PAGES**	**19a. NAME OF RESPONSIBLE PERSON**
a. REPORT	**b. ABSTRACT**	**c. THIS PAGE**			John B. Hoover
Unclassified	Unclassified	Unclassified	UL	47	**19b. TELEPHONE NUMBER** *(include area code)* (202) 767-2335

CONTENTS

1.0 BACKGROUND 1
1.1 Shipboard Storage Spaces 1

2.0 OBJECTIVES 2

3.0 EXPERIMENTAL 2
3.1 Oxygen Consumption Calorimetry 5
3.2 Test Area Description 7
3.3 Instrumentation 7
3.3.1 Calorimeter 10
3.3.2 Flow Probes 10
3.3.3 Thermocouples 10
3.3.4 Gas sampling 10
3.3.5 Optical density meters 10
3.3.6 Video 11
3.3.7 Data Acquisition System 11
3.4 Test Procedures 12
3.4.1 Calorimeter Calibration 12
3.4.2 Paper Packaging Tests 14
3.4.3 Plastic Packaging Tests 16
3.4.4 Flammable Supplies Tests 16

4.0 RESULTS 17
4.1 Data Analysis 18
4.2 Paper Packaging Tests 22
4.3 Plastic Packaging Tests 25
4.4 Flammable Supplies Tests 25

5.0 CONCLUSIONS 35

6.0 REFERENCES 36

APPENDIX A. OXYGEN CONSUMPTION CALORIMETRY A-1
1.0 DERIVATION OF EQUATIONS A-1
1.1 The Oxygen Depletion Factor A-1
1.2 The Heat Release Rate A-2
1.2.1 Complete Oxidation A-2
1.2.2 Partial Oxidation A-3
1.2.3 Wet Gas A-4
1.2.4 Final Equation A-5

APPENDIX B. TEST DATA Enclosed DVD

APPENDIX C. TEST VIDEO Enclosed DVD

1.0 BACKGROUND

The fire behavior of material found in typical storage spaces on US Navy combatants is not well understood. There are several reasons for this:

1. storage spaces contain a wide range of stock items, which range from highly flammable organic solvents[1] to non-flammable tools and machine parts;

2. a variety of packaging materials are used, which vary widely in their flammability, from steel containers to bubble wrap; and

3. fire characteristics of many of the materials involved have not been studied at full-scale or in realistic mixtures.

To address these issues, the Naval Research Laboratory (NRL) has proposed a program to investigate fire performance of real materials in typical shipboard compartments. The initial phase of the program (fiscal year 2005) addressed issues related to shipboard electronic spaces [1, 2] while the second phase (fiscal year 2006) extended the testing to dry goods storage spaces [3]. Phase two testing was accomplished at the ex-*USS Shadwell* fire test facility [4], located in Mobile, AL, during the period 11 - 21 December, 2006.

In this report, we discuss the heat release rate (HRR) for several different fire loads, including cardboard boxes, various paper products, and polyethylene bubble wrap, as measured during the December 2006 test series. It is expected that these results will prove useful for designing storage spaces for future ship classes and that the data will also provide useful benchmarks for numerical simulations using computer fire models.

1.1 Shipboard Storage Spaces

In preparation for these tests, several of the storage spaces aboard *USS Nitze* (DDG-94) were inspected to determine the types of supply items present, the stowage methods and the packaging materials used. The spaces described in Table 1 were visited, with the focus primarily on the general supply storerooms, which are the largest.

General supply spaces, shown in Figures 1 and 2 (Supply Storeroom 1), are used for storage of repair and expendable items. As seen in the figures, these spaces include drawers and shelves for small and medium sized items and a reconfigurable area for larger items and bulk supplies. In the latter area, the deck and overhead have grids of holes into which spring-loaded posts may be inserted to brace objects of almost any size or shape.

Manuscript approved March 29, 2007.

[1] Flammable organic solvents are stored in special flammable liquid store rooms and are not present in the general dry goods spaces considered in this work.

Description	Space	Types of Items
Dry Provisions Storage	2-220-2-A	Canned and boxed food stuff
Chill Storeroom	2-238-1-A	Refrigerated food storage
Freeze Storeroom	2-220-3-A	Frozen food storage
Supply Storeroom #1	3-220-01-A*	Replaceable/repairable items
HazMat Issue Room	4-410-1-A	Non-flammable hazardous items
Flammable Liquid Storage	3-410-0-K	Flammable liquids

Table 1. Major Storage Spaces on DDG-51 Class Destroyers

* There are three similar supply room (Storerooms 2 — 4) in spaces 3-346-01, 4-370-5-A and 4-370-6-A.

Items stored in these spaces include spare parts, replacement components or modules for repairable equipment and expendable supplies. Some examples, along with stowage information, are given in Table 2. Most of the parts and components are non-flammable, so the primary hazards from these items lie in the packaging materials used. Many smaller parts (such as nuts, bolts and electronic components) are packed in Kraft-type paper envelopes and stored in small drawers while medium items are in cardboard boxes, sometimes containing Kraft paper or plastic bubble wrap padding, stored on open shelves. In the bulk storage areas, most items were either relatively large individual items or cases of smaller items. For example, cases of copy paper were stored from deck to overhead (see Figure 2). Styrofoam peanuts are generally not used as packing material aboard ship. Table 3 lists some of the more common flammable materials found, either as packaging or as stock items.

2.0 OBJECTIVES

The primary objective of this test series was to measure heat release rates for typical materials found in shipboard dry goods storage spaces. A secondary objective was to obtain data sets that may be used for validation of future fire models.

It is expected that lessons learned from these tests will be applicable to future combatant designs, including the DD-1000 destroyer and the Littoral Combat Ship (LCS). The information will also be useful for developing computer models for typical types of shipboard fires.

3.0 EXPERIMENTAL

In this section, we report the experimental methodology, including a brief discussion of the theory of oxygen consumption calorimetry and descriptions of the test area, the instrumentation and the test procedures.

Figure 1. General Supply Space on *USS Nitze* (DDG-94) — Small Items

Stowage of repair parts and tools in one of the four general supply spaces aboard *USS Nitze*. Smaller items are stored in drawers while medium sized items are on shelves. Very large packages are stored as shown in the next figure.

Figure 2. General Supply Space on *USS Nitze* (DDG-94) — Large Items

Stowage of larger items (here, boxes of copy paper) in one of the four general supply spaces aboard *USS Nitze* (DDG-94). The slanted posts, which engage in the deck and overhead grids, permit the space to be configured for bulk stowage of materials having arbitrary sizes and shapes.

Typical Stock Items	Size	Stowage
Nuts, bolts, electronic components	Small	Drawers
Pipe fittings, electronic modules	Medium	Shelves
Cases of copy paper	Large	Free standing

Table 2. Stowage Examples

Typical stock items are listed, along with and indication of how they are stowed within the space.

Material	Type	Typical Stowage
Cardboard boxes & Kraft paper	Packaging material	Shelves
Cardboard boxes & bubble wrap	Packaging material	Free standing
Copy paper	Stock item	Free standing
Paper towels	Stock item	Shelves
Toilet paper	Stock item	Shelves

Table 3. Common Flammable Materials

Small, non-flammable stock items are often packed in cardboard boxes, with either paper or bubble wrap padding material, and stored on shelves. In other cases, the stock items themselves are flammable. Larger items may be stacked in an open deck area.

3.1 Oxygen Consumption Calorimetry

In classical calorimetry, a small sample is burned in a sealed vessel (commonly called a calorimetry bomb) under adiabatic conditions so that no heat is lost from the system. The temperature of the system is then measured and, from a knowledge of the system heat capacity, the energy released by the combustion may be calculated.

This method can be very accurate but is not practical for large samples, such as the contents of a compartment. Accordingly, an alternate method has been developed based on measurements of oxygen consumption during large-scale combustion processes. Although this method is not actually a form of calorimetry, the name “oxygen consumption calorimetry” has become standard.

Consider, for example, the reaction of methane with oxygen

$$CH_4 + 2O_2 = CO_2 + 2H_2O \qquad \text{Rxn. 1}$$

for which the heat of combustion is ΔH_c = 800 kJ/mol. of methane [5][2].

A key point is that the heat of combustion is defined in terms of the quantity of fuel. This makes sense, because it is normally the fuel that is the focus of interest, but it is equally possible to define the combustion energy in terms of the quantity of oxygen. The latter value would depend on the nature of the fuel so, for example, handbooks could not give the heat of combustion of oxygen as 400 kJ/mol. of oxygen. However, it has been found that, for a wide range of organic fuels, the heat released per unit of oxygen consumed is nearly constant [6], approximately 13.1 MJ/kg of oxygen.

Accordingly, it is possible to estimate the HRR of many common fires by measuring the rate at which oxygen is consumed in the combustion process. At a minimum, this method requires that the amount of oxygen be known for the supply and exhaust streams. However, the accuracy of the method may be improved by also taking into account the concentrations of carbon monoxide and carbon dioxide. Parker [7] has derived general HRR equations which may be applied to a wide range of systems and NFPA 265 [8] specifies the calorimetry methodology used in this work. A more complete explanation of the equations is given in Appendix A.

We start with the concept of the oxygen depletion factor[3], Φ, which is defined as

$$\Phi \equiv (\dot{n}^0_{O2} - \dot{n}^1_{O2}) / \dot{n}^0_{O2} \qquad \text{Eqn. 1}$$

where $\dot{n}^0_{O2}$ is the molar oxygen flow rate (mol/s) into the system (supply) and $\dot{n}^1_{O2}$ is the corresponding flow out of the system (exhaust). Equation 1 can be expressed in terms of the species volume fractions (which are the quantities actually reported by the gas analyzers), giving

$$\Phi = X^0_{O2} (1 - X^1_{CO2} - X^1_{CO}) - X^1_{O2} (1 - X^0_{CO2}) / X^0_{O2}(1 - X^1_{O2} - X^1_{CO} - X^1_{CO2}) \qquad \text{Eqn. 2}$$

where X^0_i and X^1_i are the volume fraction of species i in the supply and exhaust, respectively. HRR is determined from Φ, with corrections for incomplete combustion and water vapor, using

$$Q = \left(H_f \Phi - (H_{CO} - H_f) [(1 - \Phi)/2](X_{CO}/X_{O2})\right) (M_{O2}/M_{air}) * \left(\dot{m}^1 / [1+ \Phi(\alpha + 1)] (1 - X_{H2O}) X^0_{O2}\right) \qquad \text{Eqn. 3}$$

where Q is the HRR (in MW); H_f is the heat of combustion of fuel per mass of oxygen (13.1 MJ/kg); H_{CO} is the heat of combustion of carbon monoxide per mass of oxygen (17.6 MJ/kg); X_i is the exhaust volume fraction of species i; X^0_i is the supply volume fraction of species i; $\dot{m}^1$ is the

[2] Note that the absolute value of the heat of combustion depends on the thermodynamic states of the reactants and products. This is a complication which does not affect the arguments made here.

[3] The fraction of oxygen that has been consumed or, alternatively, the fraction of air that has been depleted of oxygen.

exhaust mass flow (in kg/s); α is a dimensionless gas expansion factor (1.105); and M_i is the molecular weight of species i (in kg/mol).

3.2 Test Area Description

An existing space[4] aboard the ex-*USS Shadwell* (01-18-3) was modified to simulate a typical *USS Arleigh Burke* (DDG-51) class dry goods storage space. Although the general supply storerooms on DDG-51 class ships have large footprints, they are subdivided into many small bays by deck-to-overhead shelves and by internal bulkheads (see Figure 1, for example). As a consequence, a relatively small mockup provides a realistic simulation of the conditions found in a DDG-51 storage space.

The area selected for the mockup is adjacent to the pre-existing oxygen consumption calorimeter, located in space 01-15-3, which permits estimation of HRR. Figure 3 shows the combined fire test and calorimetry areas, with the dashed box indicating the approximate location of the overhead exhaust hood within the calorimeter area.

Five pairs of shelves were installed in the test area, four of them in two back-to-back sets (1A — 4B in Figure 3). All of the shelves were assembled from commercial sheet metal components obtained from Shelving Unlimited, Inc. All, except for units 4A and 4B, had solid shelves, backs and sides. Units 4A and 4B lacked the side walls, but were otherwise identical.

This layout provided tall storage units, separated by aisles, similar to the arrangement of DDG-51 dry goods storerooms. Combustible materials were located on shelves 2A and 2B (for small and medium size boxes) or in the area indicated by the dotted square (for large boxes). The placement of the remaining shelves was designed to channel air flow from the entrance, through the fire area, and out to the calorimeter, as indicated by the curving arrow in the Figure. Details of the fuel loads and locations for each test are discussed below.

3.3 Instrumentation

Because the primary goal of these tests was to estimate the HRR for each of the fuel loads, the calorimeter was the most critical system. In addition to the calorimeter, instruments were provided to collect environmental data in the storage space that can be used in the future for fire model validations. The environmental instruments, which are indicated in Figure 4, included:

1. Flow probes to measure air flow into and out of the space;
2. Thermocouple trees to monitor air temperatures as a function of elevation;
3. “Package” thermocouples to measure flame temperatures and surface temperatures of test items;
4. Gas sampling intakes;
5. Optical density meters (ODMs); and
6. Thermal imaging and visible light video cameras to record the development of the fires.

[4] This space was previously used for studies of berthing space materials [9].

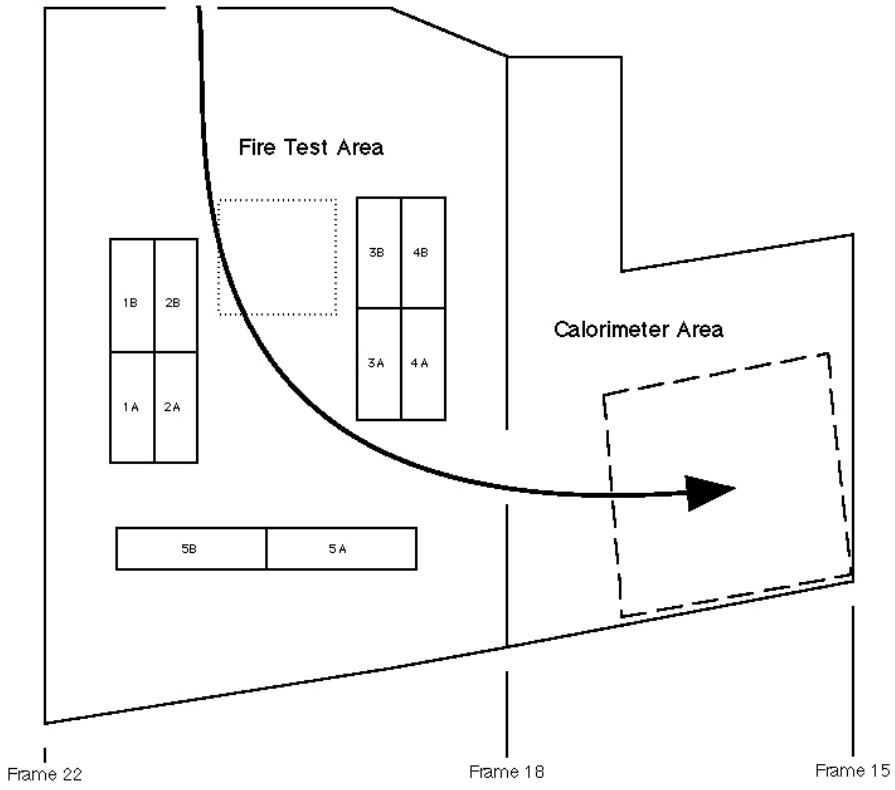

Figure 3. Test Area Layout

The mockup supply space provides both shelves (solid outlines) and a bulk storage area (dotted outline) and is adjacent to the oxygen consumption calorimeter space. The curved arrow indicates the approximate air flow though the test area and into the calorimeter area.

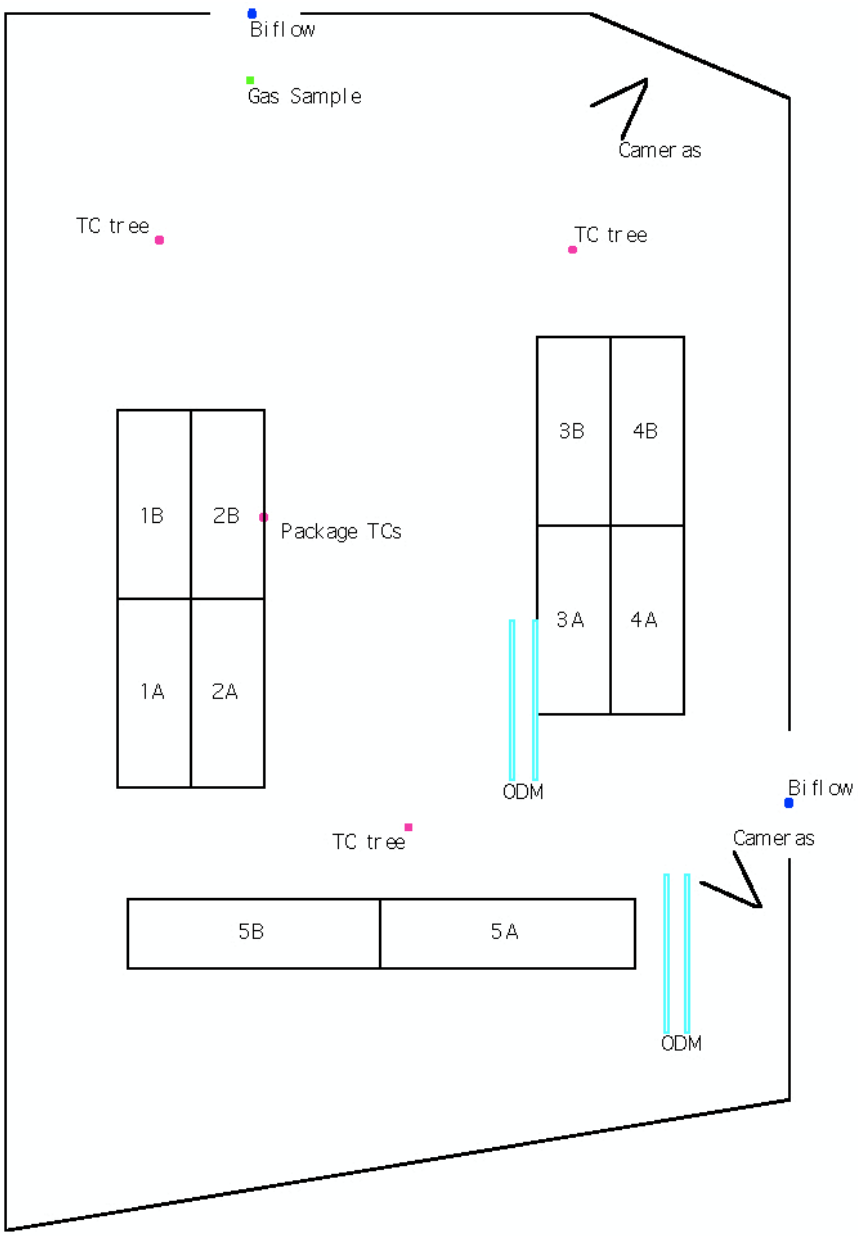

Figure 4. Instrumentation Layout for the Storage Space Mockup

Approximate instrument locations within the simulated general supply storage space are shown in this diagram. The “V” at the two camera positions indicates the approximate field of view.

3.3.1 Calorimeter

The calorimeter system included an exhaust hood, located in the overhead of the calorimeter space (see Figure 3), an instrumented duct (shown in Figure 5) to monitor combustion products and an exhaust blower that ensures that all fire products are captured.

Within the duct, a thermocouple and flow probe provide temperature and volume flow rates, from which mass flow rates may be calculated. Measurements at multiple points within the exhaust duct confirmed that the flow was nearly independent of location, so a single flow probe located on the centerline was sufficient. The hoop-shaped gas probe sampled from multiple locations, which has the effect of averaging the concentrations of oxygen, carbon dioxide and carbon monoxide across the duct.

3.3.2 Flow probes

Two bi-flow probes were installed at different elevations on the centerlines of each entrance to the test compartment. These devices measure the volume flow rate, in either direction, through the openings.

3.3.3 Thermocouples

Three thermocouple trees, each consisting of five type K thermocouples spaced at intervals of approximately 0.6 m (2 ft), were suspended from the overhead to provide vertical temperature profiles in the space. Two individual thermocouples were used to monitor the surface temperatures of selected fuel items. Thermocouples were also collocated with each of the bi-flow probes discussed in the section above.

3.3.4 Gas sampling

Two gas sampling points were located within the test area while the third was inside the calorimeter duct, as described above. Each gas sampling loop included a filter and a cold trap to remove particulates and condensible gases (primarily, water vapor). The clean, dry gas then flowed through analyzers which measured the concentrations of oxygen, carbon monoxide and carbon dioxide in each sample stream. Analyzer outputs were digitized and stored for later analysis.

3.3.5 Optical density meters (ODMs)

Four ODMs were installed on two different levels at each of the two locations shown in Figure 4. The lower level instruments were approximately 0.6 m (2 feet) above the deck while the upper ones were located about 1.8 m (6 feet) above the deck. These elevations were selected to represent head heights for crawling and standing persons, respectively.

The ODMs used low power lasers to monitor optical transmittance over a path length of approximately one meter. This signal, which is inversely related to the amount of soot in the air, provided an estimate of the degree of obscuration caused by the soot [10].

Figure 5. Interior of Calorimeter Exhaust Duct

The calorimeter gas intake is a hoop-shaped length of stainless steel tubing with multiple holes which sample a cross section of the flow. The small cylinder on the centerline of the duct, above the gas intake, is a biflow probe that measures flow velocity. The temperature monitoring system is not visible from this angle.

3.3.6 Video

One infrared/low light and one visible light video camera were installed near each of the two locations shown in Figure 4. The locations, which were chosen to provide coverage of the ignition source and the main fire, were changed several times during tests, depending on the fire location and expected fire size, to get the best view while minimizing the risk of thermal damage to the cameras.

3.3.7 Data acquisition system

The data acquisition system consisted of a computer, running custom National Instruments (NI) LabVIEW software, which remotely managed a chassis containing NI compact FieldPoint modules that digitized the instrument signals. The digitized data were then sent back to the control computer, where they were logged, scaled according to the calibration curve for the specific instrument and saved onto disk for later analysis.

The primary advantage of this system over the previously-used MassComp system is that digitization occurs much closer to the instrument location and, therefore, the signal-to-noise ratio is expected to be significantly improved. This system also made it easier to change the instrument configuration — most such changes only required that the instrument connection at the FieldPoint module be changed and that the corresponding configuration file on the control computer be updated.

3.4 Test Procedures

Four series of tests, described in Table 4, were carried out during this test program and, in addition, calibration and shakedown tests were conducted with a propane gas burner and with several sizes of heptane pan fires. Many of the tests were repeated in order to gather statistical information needed to evaluate the reproducibility of the work. Procedures used for all tests are discussed below.

For each test and for the heptane calibrations, data were collected for a period of approximately two minutes prior to ignition in order to establish background levels for the measured parameters. At the end of this "pre-burn" time, the heptane pool fire was manually ignited and, in the case of the materials tests, this heptane pilot fire ignited the actual test materials.

Test Series	Types of Materials	Fuel
B&P	Paper Packaging	Small cardboard boxes w/ crumpled Kraft paper padding.
B&BW	Plastic Packaging	Large cardboard boxes w/ polyethylene bubble wrap padding.
PT & TP	Paper Supplies	Cases of paper towels and toilet paper.
CP	Paper Supplies	Cases of copy paper.

Table 4. Test Series Descriptions

The four test types are listed, along with the general classification of the materials and the specific fuel used in each.

3.4.1 Calorimeter calibration

An initial calibration of the calorimeter system was carried out under standard conditions in which a propane fired sand burner was located immediately below the exhaust hood in the calorimeter space. Propane was supplied from a liquid storage tank and the gas flow was regulated using a rotameter (Barnant model GF-1660 with a #5 flow tube or King Instruments model 7530-2-1-1-7C-07, depending on the flow rate). A needle value, upstream of the rotameter, was used to control the flow and the readings were corrected for the flow tube internal pressure, which was measured immediately downstream of the rotameter. Heat release rates were calculated using the known heat of combustion of propane (46.45 MJ/kg) [5].

The actual materials tests were conducted in the adjoining test space, rather than in the calorimeter space, and it was found that the method described above was not able to calibrate the calorimeter above about 300 kW, due to limitations on the propane flow rate. To correct for the change in fire location and to extend the calibration range, additional calibrations were carried out using heptane pool fires of various sizes as secondary standards. The first series of heptane pool fires, up to approximately 680 kW, was set in the calorimeter space (as shown in Figure 6).

Figure 6. Series 1 Heptane Pool Calibration Fire

This heptane pool fire (nominally 110 kW) was one of a series, carried out in the calorimeter space, used to establish a set of secondary standard. The fire pan is resting on the sand burner used for the propane fires.

Subsequently, the same pool fires were repeated in the test space, with the pan located next to shelf unit 2B (Figure 7).

Figure 7. Series 2 Heptane Pool Calibration Fire

> The heptane pool fire shown in the previous Figure was repeated in the test space to compensate for the effects of the different fire location.

Using the initial (propane) calibration, the actual sizes of the heptane pool fires were calculated based on the calorimeter space pool fires; these secondary calibration standards were then used to establish the calorimeter's response to fires within the test space and this final calibration was used to calculate the sizes of the test fires.

3.4.2 Paper packaging tests

The paper packaging tests were designated as the box and paper (B&P) series. For these tests, the fuel load was composed of various numbers of 30.5 cm x 30.5 cm x 15.2 cm (12 in. x 12 in. x 6 in.) cardboard boxes (Uline corrugated cardboard boxes, S-4122), each filled with 20 sheets of crumpled 30.5 cm x 30.5 cm (12 in. x 12 in.) wrapping paper (Uline 50 lb Kraft paper, S-11421) and sealed with 5 cm (2 in.) transparent tape. A single fuel package is shown in Figure 8A and 8B before and after sealing.

Figure 8. Fuel Package for B&P Tests

One box of the type used in the B&P test series is shown. Up to 57 of these packages were used in a single test.

All of these tests used the same 21.6 cm x 21.6 cm (8.5 in. x 8.5 in.) pan that was used for the secondary standardization fires. In tests B&P-01 and B&P-02, a methanol fire was used as the ignition source in order to minimize interference with the test fires due to the production of smoke. Two different pilot fire configurations were tried, but it was found that these methanol fires were not sufficiently energetic to ignite the boxes. Accordingly, for all of the remaining tests, heptane was used for the ignition source, with the pan located at the forward, port corner of either shelf unit 2B or 2A (see Figure 4 for locations). This location was chosen because the ventilation system (which was required for the calorimeter) caused the flames to tilt to starboard. Thus, placing the ignition source at the port corner of the fuel load ensured that the flames were drawn toward, rather than away from, the test materials.

During test B&P-05, it was found that horizontal fire spread from one shelf unit to another was severely limited and, in order to improve the probability of ignition of both shelf units, the pilot fire was moved to the junction of units 2A and 2B (forward, port corner of unit 2A).

3.4.3 Plastic packaging tests

The basic fuel package for the box and bubble wrap (B&BW) series was a 1.22 m x 0.61 m x 0.61 m (48 in. x 24 in. x 24 in.) cardboard box (Uline corrugated cardboard boxes, S-4749) containing a 7.6 m x 1.22 m (25 ft x 48 in.) sheet of polyethylene bubble wrap having 1.3 cm (0.5 in.) bubbles (Uline Economy Bubble Wrap, S-3932P). Figure 9 shows one package prior to sealing with 5 cm (2 in.) transparent tape.

Each test used four fuel packages, arranged in a two-by-two stack in the space between shelf units 2B and 3B. Ignition of the test materials was accomplished using the 21.6 cm x 21.6 cm (8.5 in. x 8.5 in.) pan, charged with 0.5 l (0.13 gal) of heptane, placed adjacent to the aft, port corner of the fuel stack.

3.4.4 Flammable supplies tests

Unlike the packaging tests discussed above, the paper supplies tests focused on supply items that are inherently flammable. Within this category, two sets of tests were conducted: one using loosely packed items and the other using densely packed material. The former, designated as the PT&TP series, involved cases of paper towels (ProLink Green, RH-626) or toilet paper (ProLink 2-ply tissue, RR202-LH) while the latter (the CP series) used cases of standard copy paper (Boise Aspen, white, 20 lb) for the fuel loads.

In the PT&TP series, two preliminary tests were conducted, one each with paper towels and toilet paper alone, while the remaining three tests used a combination of both items. The fuel load was arranged with cases of toilet paper on shelf unit 2A and paper towels on unit 2B. In the preliminary tests, only one shelf unit was used for each test — unit 2A for test TP-01 and 2B for PT-01. For the combined item tests and for the toilet paper test, the heptane pilot fire was located between the two shelf units, near the forward, port corner of shelf unit 2A; for the paper towel test, it was located at the forward, port corner of shelf unit 2B.

Figure 9. Fuel Package for B&BW Tests

One box of the type used in the B&BW test series is shown. Each box was 0.61 m x 0.61 m x 1.22 m (24 in. x 24 in. x 48 in.) and contained 25 ft of bubble wrap.

For these tests, the spacing of the shelves in unit 2A was changed relative to the configuration used during the B&P series. The bottom shelf on unit 2A was removed and the other two were lowered to provide sufficient space for the large cases used in this test series.

One CP test was carried out and, for that test, five cases of copy paper were placed in the area between shelf units 2B and 3B, in the same space used for the B&BW tests. Three cases were placed on the deck and the other two cases were stacked on top. The heptane pan was located near the aft, port corner of the stack.

4.0 RESULTS

In this section, we first present the methods used to analyze the test data, followed by a discussion of the results obtained for each test series. The approximate fuel load for each test article, calculated from the vendor's data, is given in Table 5. These values were used to estimate total fuel masses, which appear in subsequent tables.

The raw data from these tests are given in Appendix B and examples of the visible light video may be found in Appendix C. Both of these Appendices are on the included DVD disk.

Test Article	Unit	Mass [kg (lb)]
Box & paper	Box	0.51 (1.1)
Box & bubble wrap	Box	3.5 (7.7)
Toilet paper	Case	18 (40)
Paper towels	Case	10 (23)
Copy paper	Case	23 (50)

Table 5. Approximate Test Articles Fuel Masses

4.1 Data Analysis

Several factors complicated the data analysis. First, the propane and pool fires had vastly different time curves, which raised questions regarding the best way to define the fire size. The second factor was the impact of the calorimeter detection limit for test space fires.

Typical time histories for similarly sized propane and heptane fires are illustrated in Figure 10. For propane fires, the HRR rose almost instantly to the peak value, stayed at that level for the duration of the test and immediately dropped to zero at the end of the test. In contrast, the heptane fires ramped up rather slowly, continuing to increase during most of the test and dropped off sharply (but not as quickly as the propane fires) when the fuel burned out.

The easiest method for estimating HRR would have been to take the average over the test time. However, this clearly would have given misleading results, since the pool fires (and the materials test fires) were well below their maximum HRR values for much of the test period. Also, some of the materials fires continued to burn for an extended period and, ultimately, had to be extinguished, making the definition of "test time" somewhat arbitrary. Alternatively, we could have taken the maximum value, but this method would have been very sensitive to random test-to-test variations.

To address the time history problem, a standard method was developed to specify the period over which the average should be taken and to process the data for this period. A 20-point sliding average (corresponding to 20 seconds) was applied to remove most of the noise spikes; the background average and standard deviation were calculated from the smoothed data. The period during which the fire consistently exceeded the background by two standard deviations[5] was considered to be the test period. The background mean was subtracted from the data and the zero time was shifted to correspond to the start of the test period. The peak value was then visually estimated and all values greater than 90% of the estimated peak were averaged to obtain a measure of the maximum HRR for the fire.

[5] This approximately corresponds to a 95% confidence interval.

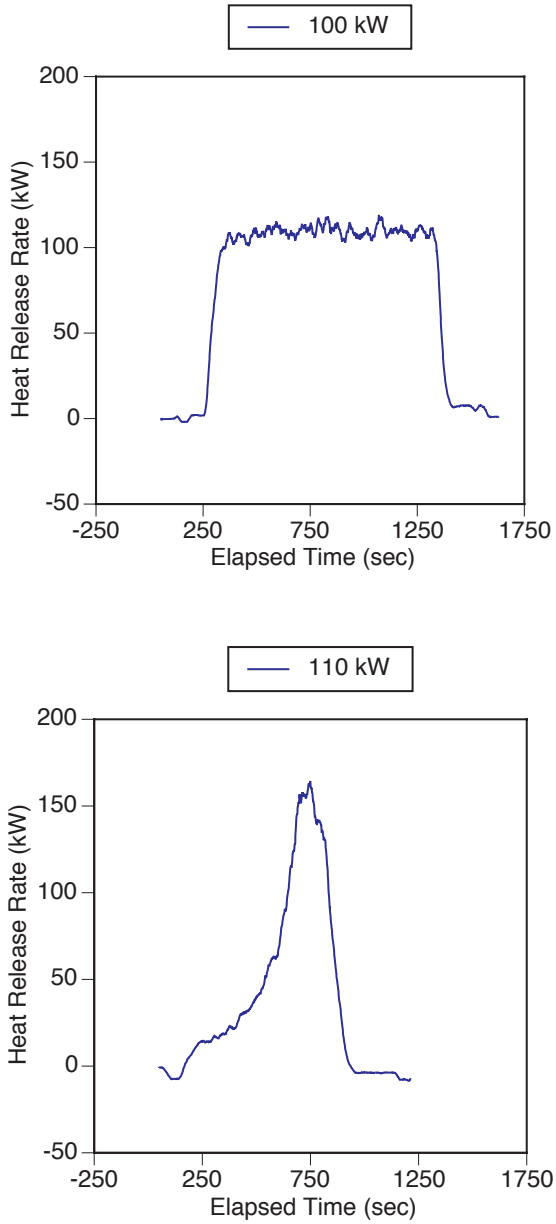

Figure 10. Comparison of Propane and Heptane Fires

Typical propane (upper) and heptane (lower) fires, both with nominal HRR values of approximately 100 kW, have very different time curves.

This method is less sensitive to random variations than is the maximum value method and is more indicative of the worst case fire threat than is the mean value method. However, the choice of the 90% threshold is arbitrary and, as a check, the same procedures were carried out using a threshold of 75%. For example, the heptane data from Figure 10 was processed using both thresholds. The results are shown in Figure 11, where the solid line is the portion of the curve that exceeds the 75% threshold and the shaded line is the region above 90%. The HRR values calculated with these two thresholds (146 kW and 154 kW, respectively) differ by about 5%, indicating that this method is relatively insensitive to the value of the threshold parameter.

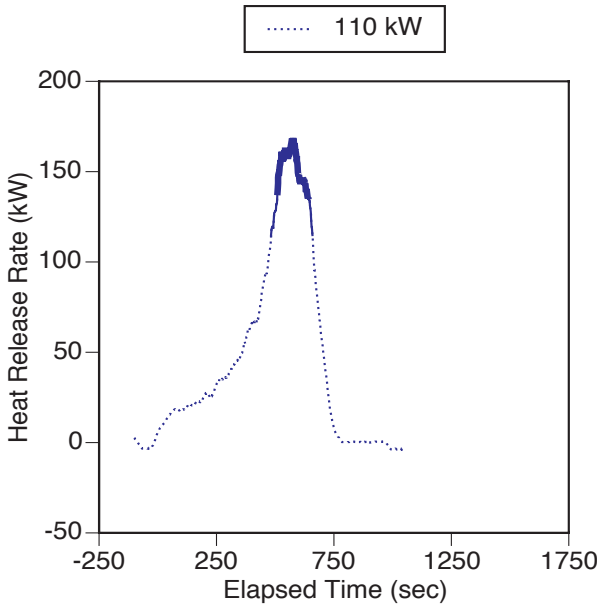

Figure 11. Data Processing Results

The data from the nominal 110 kW heptane fire (dotted line) have been processed using the method described in the text. The solid region corresponds to the 75% threshold and the bold segment to 90%.

The initial calorimeter calibration curve is shown in Figure 12, where the propane flow rates were adjusted to give HRR values of 50, 100, 250 and 300 kW and the data were processed using both thresholds. The close correlation of the two sets of results is further evidence that the analysis method is insensitive to the choice of threshold.

A linear fit to the data was calculated (solid curve in Figure 12); the inverse of this function was the calorimeter calibration for standard conditions. The sizes of the secondary standard fires (heptane pool fires located within the calorimeter space) were calculated using this calibration and are reported in Table 6. For the remainder of this discussion, only the results obtained with the 90% threshold are reported.

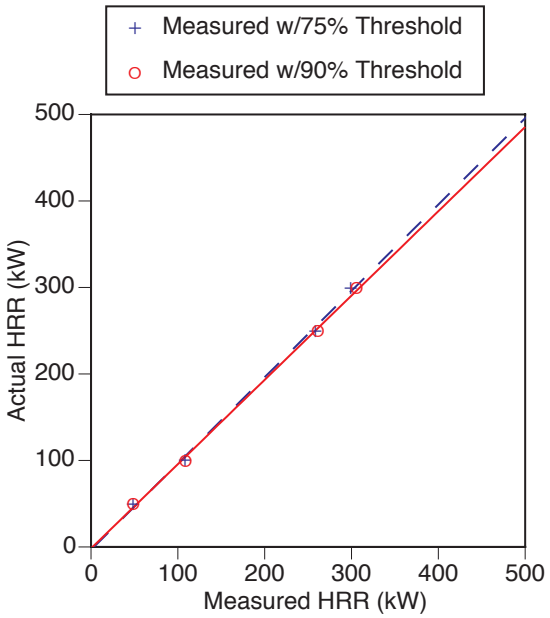

Figure 12. Initial Calorimeter Calibration

The calorimeter system was initially calibrated using propane gas fires. Data were processed, as described in the text, and the peak region was determined using two different thresholds (dashed line for 75% and solid line for 90%). The actual HRR was calculated from the calorimeter output under standard conditions, using the 90% threshold curve.

Pool Dimensions	**Calculated HRR (kW)**
15.2 cm (6.0 in.) diam.	42.17
21.6 cm x 21.6 cm (8.5 in. x 8.5 in.)	147.89
26.7 cm x 26.7 cm (10.5 in. x 10.5 in.)	251.32
61.0 cm (24 in.) diam.	796.94

Table 6. Secondary Standard Heat Release Rates

As described in the text, these heptane pools fires were used as secondary standards to correct for the differences between fires in the calorimeter space and those in the test space.

The corrected calibration curve, based on the secondary standards, is shown in Figure 13. Note that the calibration does not go through zero. This is due to the non-zero detection limit of the system — any fire less than this limit produces a zero output. It is likely that the calibration curve becomes non-linear for small fires so that the linear extrapolation overestimates the HRR for these fires.

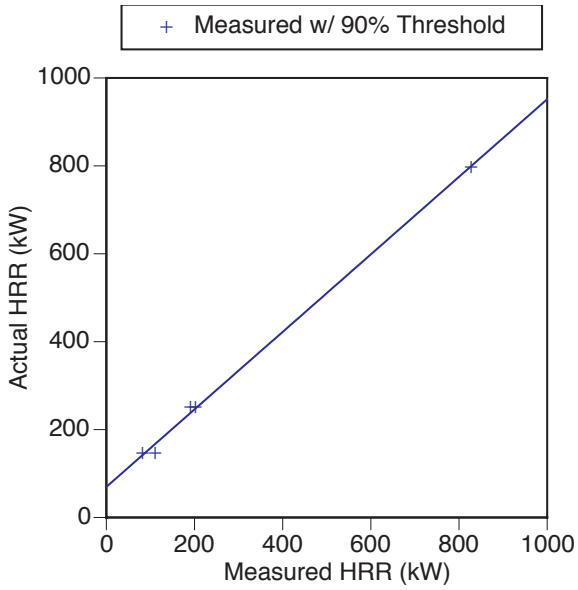

Figure 13. Corrected Calorimeter Calibration

The initial calorimeter calibration was corrected for the differences between fires in the calorimeter space and those in the actual test area using heptane pool fires as secondary standards.

4.2 Paper Packaging Tests

The number and layout of the boxes in the B&P tests are listed in Table 7. The fuel layout column in this Table gives the number of boxes on each shelf, from the lowest shelf to the highest. In B&P-03, there was a single column of three boxes; in all other tests, there were three columns. As an example, the full fire load (54 boxes) for test B&P-05 is shown in Figure 14. For comparison, post-test photographs for tests B&P-05 (top) and B&P-06 (bottom) are shown in Figure 15. There is a significant amount of ash, which indicates that, even when the boxes burned, not all of the material was consumed. Note that the heptane pan used for the pilot fire is visible near the lower, right corner of the lower photograph in Figure 15.

During test B&P-05, it was found that the materials in shelf unit 2B were completely consumed but those in 2A never ignited. This was attributed to the facts that the pilot fire directly impinged on the boxes in unit 2B whereas those in unit 2A were not directly exposed to flames and the steel shelf side walls severely limited horizontal fire spread from one shelf unit to another, even though the barrier was very conductive. The partial ignition failure during the last test is believed to have been due to the flames having been pulled away from unit 2B by the forced ventilation.

Table 8 lists the peak HRR for each test in this series, calculated as described above. It includes the number of boxes actually burned and the estimated fuel mass. The latter was based on the mass of the individual test articles, as previously discussed. The variation in the HRR calculated for replicate tests is largely attributable to variations in the fraction of the fuel load that was actually consumed.

Test	Heptane Load [l (gal)]	Ignition Location	Fuel Load (boxes)	Fuel Layout	Fuel Burned (boxes)
B&P-03	0.5 (0.13)	Unit 2B	3	3 (vertical)	3
B&P-04	0.5 (0.13)	Unit 2B	27	9,6,6,6	27
B&P-05	0.25 (0.07)	Unit 2B	54	2 x 9,6,6,6	27*
B&P-06	0.25 (0.07)	Unit 2A	54	2 x 9,6,6,6	54
B&P-07	0.25 (0.07)	Unit 2A	54	2 x 9,6,6,6	27**

Table 7. Test Descriptions - B&P Paper Packaging Tests

The ignition source was the 21.6 cm x 21.6 cm (8.5 in. x 8.5 in.) pan, filled with the volume of heptane shown. The pan was located at the forward, port corner of the indicated shelf unit (see Figure 4). The layout column gives the number of boxes on each shelf, listed from bottom to top.

* No ignition in unit 2A.
** No ignition. in unit 2B.

Figure 14. B&P Test Series Fuel Layout

The fuel layout for test B&P-05, shown prior to the start of the test. Shelf unit 2A is on the left and 2B on the right.

Figure 15. Post-Test B&P Test Series Results

The upper photograph shows the results of the B&P-05 test, in which only half of the fuel load burned. In the lower photograph, from B&P-06, the entire load burned. There was a significant amount of ash left after the fire burned out.

Test	Fuel Load (boxes)	Mass Burned [kg (lb)]	Peak HRR (kW)
B&P-03	3	1.5 (3.4)	169
B&P-04	27	13.8 (30.5)	548
B&P-05	27	13.8 (30.5)	506
B&P-06	54	27.5 (61.0)	921
B&P-07	27	13.8 (30.5)	390

Table 8. Peak Heat Release Rates - B&P Paper Packaging Tests

The peak HRR values, calculated as described in the text, are listed for each of the B&P series tests. The fuel load is the number of boxes actually burned, not the original number.

4.3 Plastic Packaging Tests

The box and bubble wrap (B&BW) series consisted of the two replicate tests described in Table 9. As seen in Figure 16, each test used four fuel packages and the pilot fire was located adjacent to the aft, port corner of the fuel stack.

Test	Heptane Load [l (gal)]	Ignition Location	Fuel Load (boxes)	Fuel Layout	Fuel Burned (boxes)
B&BW-01	0.5 (0.13)	Stack	4	2,2	4
B&BW-02	0.25 (0.07)	Stack	4	2,2	4

Table 9. Test Descriptions - B&BW Plastic Packaging Tests

The ignition source was the 21.6 cm x 21.6 cm (8.5 in. x 8.5 in.) heptane pool fire, which was located at the aft, port corner of the stack of boxes. For each test, there were two layers of two boxes.

The HRRs from the two replicate tests were in very good agreement, differing by less then 2%, and there was almost total destruction of the test material, as indicated by the lack of ash visible in the post-test photograph (Figure 17). Combustion of the polyethylene bubble wrap was very exothermic and, as a result, the HRR was very high as shown by the HRR values given in Table 10.

4.4 Flammable Supplies Tests

The fuel loads used in the PT&TP tests are given in Table 11 and the packages were arranged as shown in Figure 18. As mentioned above, the boxes on the left shelves (unit 2A) were the large cases of toilet paper; those on the right (unit 2B) were paper towels. During the preliminary tests, the fuel load was as shown except that items were placed only on unit 2A (TP-01) or 2B (PT-01).

Figure 16. B&BW Test Series Fuel Layout

The fuel load for test B&BW-01 consisted of four of the boxes shown in the previous figure. The fire pan for the heptane ignition source is visible at the lower right corner.

Figure 17. Post-Test B&BW Test Series Results

Due to the high flammability of the polyethylene bubble wrap, the B&BW test articles were completely incinerated, leaving almost no ash at the end of the tests.

Test	Fuel Load (boxes)	Mass Burned [kg (lb)]	Peak HRR (kW)
B&BW-01	4	14.0 (30.8)	1090
B&BW-02	4	14.0 (30.8)	1071

Table 10. Peak Heat Release Rates - B&BW Plastic Packaging Tests

The peak HRR values, calculated as described in the text, are listed for each of the B&BW series tests. The fuel load is the number of boxes that actually burned.

Test	Heptane Load [l / (gal)]	Ignition Location	Fuel Load (cases)	Fuel Layout	Fuel Burned (cases*)
PT-01	0.5 (0.13)	Unit 2B	10	4,2,2,2	10
TP-01	0.5 (0.13)	Unit 2A	3	1,1,1	3
PT&TP-01	0.5 (0.13)	Unit 2B Unit 2A	10 3	4,2,2,2 1,1,1	10 3
PT&TP-02	0.25 (0.07)	Unit 2B Unit 2A	10 3	4,2,2,2 1,1,1	10 3
PT&TP-03	0.25 (0.07)	Unit 2B Unit 2A	10 3	4,2,2,2 1,1,1	10 3

Table 11. Test Descriptions - PT&TP Flammable Supplies Tests

The ignition source was the 21.6 cm x 21.6 cm (8.5 in. x 8.5 in.) pan, filled with the volume of heptane shown. The pan was located at the forward, port corner of the indicated shelf unit. The layout gives the number of boxes on each shelf, listed from bottom to top.

* Significant quantities of these test materials were unburned at the end of the tests.

Figure 18. PT&TP Test Series Fuel Layout

> For the combined paper towel and toilet paper fires, the test items were loaded on adjacent shelf units (2B and 2A, respectively). For tests of individual items, the cases were in the locations shown, but only one shelf unit was used for each test.

Figure 19 shows the post-test conditions at the conclusion of one of these tests. It was found that, after the cardboard packing cases burned through, many of the rolls of toilet paper and bundles of paper towels fell onto the deck and continued to burn. Also, the paper towel bundles were compressed by a paper retaining band and, when this band burned, the bundles burst and spread burning debris onto the deck. Due to the lack of oxygen circulation within the debris pile, a significant quantity of material smoldered or charred but did not burn, as seen in Figure 20. HRRs for these tests are reported in Table 12.

Only one CP test was carried out, as described in Table 13, with the cases stacked as shown in Figure 21. For this test, the heptane pan was located near the aft, port corner of the stack (the lower right corner of Figure 21). As might be expected, the densely packed reams of paper proved difficult to ignite and burned poorly, due to the lack of air circulation within the fuel load. All but one of the cardboard packing cases did burn to ash, as seen in the post-test photograph, Figure 22. The calculated HRR for CP-01 is given in Table 14.

Figure 19. Post-Test PT&TP Test Series Results

There was a large quantity of ash and unburned material left after these tests. Also, after the cardboard packing cases burned, the enclosed items (particularly the paper towels) spilled onto the deck.

Figure 20. Unburned PT&TP Test Material

This close-up shows that much of the residual paper towel material was not burned.

Test	Fuel Load (cases)	Mass Burned [kg (lb)]	Peak HRR (kW)
PT-01	10 PT	104 (230)	299
TP-01	3 TP	54.3 (120)	628
PT&TP-01	10 PT + 3 TP	158 (350)	788
PT&TP-02	10 PT + 3 TP	158 (350)	774
PT&TP-03	10 PT + 3 TP	158 (350)	666

Table 12. Peak Heat Release Rates - PT&TP Flammable Supplies Tests

The peak HRR values, calculated as described in the text, are listed for each of the PT&TP series tests. The fuel load is the number of cases of paper towels (PT) and toilet paper (TP) that actually burned. Note that, as discussed in the text, combustion was not complete.

Test	Heptane Load [l (gal)]	Ignition Location	Fuel Load (cases)	Fuel Layout	Fuel Burned (cases*)
CP-01	0.5 (0.13)	Stack	5	3,2	4

Table 13. Test Descriptions - CP Flammable Supplies Test

The ignition source was the 21.6 cm x 21.6 cm (8.5 in. x 8.5 in.) pan with 0.25 l (0.07 gal.) heptane. The pan was located at the forward, port corner of the cases, which were stacked with three cases on the lower layer and two on the upper.

* Four of the cardboard cases were nearly totally consumed, but almost none of the paper burned.

Figure 21. CP-01 Test Fuel Layout

The five cases of copy paper were stacked in the same location used for the B&BW tests. A portion of the heptane pan is visible in the lower, right corner of the photograph.

Figure 22. Post-Test CP Test Series Results

The copy paper proved very resistant to fire, as seen in this photograph. The visible ash is from the cardboard cases (note the unburned case at the left).

Test	Fuel Load (boxes)	Mass Burned [kg (lb)]	Peak HRR (kW)
CP-01	5	114 (230)	178

Table 14. Peak Heat Release Rates - CP Flammable Supplies Test

The peak HRR value, calculated as described in the text, for the CP series test. The fuel load is the number of cases that actually burned, but note that very little of the material was actually consumed.

5.0 CONCLUSIONS

As was shown in the preceding tables, peak heat release rates for typical shipboard general storage space materials vary widely, depending on both the quantity and type of combustible material. In Figure 23, these peak HRR values were plotted, as a function of the fuel load, for each of these tests. It was found that the tests fall into four general categories, as indicated by the lines superimposed on the data points in Figure 23.

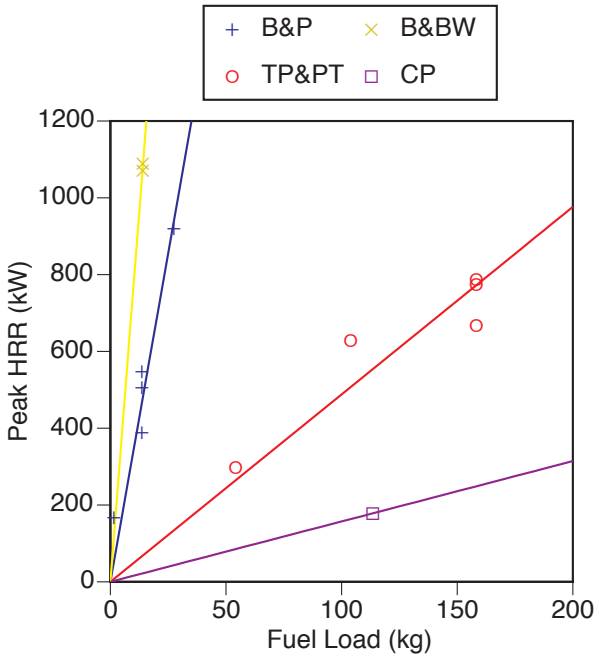

Figure 23. Peak Heat Release Rates

The peak HRRs for the four different types of fuel load are plotted as a function of the mass of the load.

For the B&P, TP&PT and CP tests, the nature of the materials involved was very similar. Consequently, the differences in fire behavior are largely due to the differences in the fraction of the fuel load that was actually consumed. That, in turn, was attributable to the differences in packing density which was a controlling factor for oxygen circulation within the fire.

These results show a trend in which the HRR per unit fuel mass is inversely related to the amount of residual fuel. This is in qualitative agreement with the observed quantities of residual ash: relatively little ash in the B&P tests corresponds to a steep slope while large quantities of unburned material in the CP test corresponds to a shallow slope.

As was seen in Figure 17, the B&BW tests produced almost no residual ash, which is also consistent with the observed trend. However, in this case, the primary cause of the markedly higher HRR per unit fuel mass is probably the nature of the material — the heat of combustion of polyethylene is almost three times greater than that of paper.

We note that the lines shown in Figure 23 were forced to go through zero and therefore do not reflect a least squares curve fit to the data. In the B&BW and CP tests, only a single fire size was used so there is insufficient data for a curve fit. For the other cases, the previously discussed detection limit issue makes extrapolation to small HRR values inaccurate.

However, the lines are reasonable approximations for estimating peak HRR of two classes of materials found in general storage spaces: paper products and polyethylene plastics. For both classes, the effects of fuel load can be estimated and, for the former, guidance regarding the effects of packing density on HRR is provided. Approximate values for HRR per unit mass are given in Table 15 and may be useful for computer modeling of storage space fires.

Test Series	**Primary Material Type**	**Packing Density**	**Peak HRR per Unit Mass (kW / kg)**
B&BW	Plastic	Low	77.2
B&P	Paper	Low	34.2
TP&PT	Paper	Medium	4.9
CP	Paper	High	1.6

Table 15. Approximate Peak HRR vs. Mass

The values listed in the last column were estimated from the slopes of the peak HRR versus fuel load graphs.

6.0 REFERENCES

1. J.B. Hoover, C.L. Whitehurst, E.B. Chang and F.W. Williams, “Report of Fire Performance of Shipboard Electronic Space Materials,” NRL Letter Report 6180/0007, 12 January 2006.

2. J.B. Hoover, C.L. Whitehurst, E.B. Chang and F.W. Williams, "Final Report on Fire Performance of Shipboard Electronic Space Materials," NRL Memo Report NRL/MR/6180--06-8983, 15 September 2006.

3. J.B. Hoover and F.W. Williams, "Test Plan: Fire Performance of Shipboard Electronic Space Materials," NRL Letter Report 6180/0172, 8 August 2006.

4. H.W. Carhart, T.A. Toomey and F.W. Williams, "The ex-USS SHADWELL Full-Scale Fire Research Test Ship," NRL Memo Report NRL/MR/6180--87-6074, 6 October 1987.

5. D. Drysdale, "Heats of Combustion of Selected Fuels at 25°C," Table 1-10.3 in "SFPE Handbook of Fire Protection Engineering," Soc. Fire Prot. Eng., 1st Ed., 1988.

6. C. Huggett, "Estimation of Rate of Heat Release by Means of Oxygen Consumption Measurements," Fire & Materials, **4**, 61, 1980.

7. W.J. Parker, "Calculation of the Heat Release Rate by Oxygen Consumption for Various Applications," NIST Report NBSIR 81-2427-1, March 1982.

8. National Fire Protection Association, "Standard Methods of Fire Tests for Evaluating Room Fire Growth Contribution of Textile Wall Coverings," NFPA 265, 1988.

9. F.W. Williams, J.J. Beitel, B.J. Havlovick, D.T. Gottuk and M. Peatross, "Analysis of Small-Scale and Real-Scale PFP Test," NRL Letter Report 6180/0194, 2 May 1994 .

10. M.J. Ferreira, J.L. Scheffey, S.A. Hill, P.A. Tatem and F.W. Williams, "Comparison of Visibility Distance Correlations with Recent Full-Scale Test Data," NRL Letter Report 6180/0690, 31 December 1997.

ACKNOWLEDGMENTS

We would like to thank LT Cycyk, SECONDFLT scheduling office, for scheduling a ship visit, and the crew of *USS Nitze* (DDG-94) for their hospitality during a very informative ship visit. Special thanks go to LT Allen (Operations Officer, *USS Nitze*), for arranging the visit clearance, and to LT Hamilton (Supply Officer, *USS Nitze*), who took time to answer questions regarding the operations of the Supply Division.

This work would not have been possible without the hard work of the crew of the ex-*USS Shadwell*. In particular, we wish to thank An Nguyen, Arthur Durkin, Manton Smith, Robert Burgess, Russell Robertson, Ford Le, CWO3 John Hopson, MMPO3 Michael Jackson and Vonnie Byrd. Thanks also to Jean Bailey for her helpful suggestions during the preparation of this manuscript.

APPENDIX A. OXYGEN CONSUMPTION CALORIMETRY

1.0 DERIVATION OF EQUATIONS

The equations used for oxygen consumption calorimetry were presented in section 3.1 of the report. In this appendix, we provide additional information and present a derivation of those equations in order that the assumptions involved may be understood.

1.1 The Oxygen Depletion Factor

As discussed in the body of this report, the oxygen depletion factor, Φ, is defined as

$$\Phi \equiv (\dot{n}^0_{O2} - \dot{n}^1_{O2}) \diagup \dot{n}^0_{O2} \qquad \text{Eqn. A1}$$

where $\dot{n}^0_{O2}$ is the molar oxygen flow rate (mol/s) into the system (supply) and $\dot{n}^1_{O2}$ is the corresponding flow out of the system (exhaust).

We define the mole fraction of species i to be

$$X_i \equiv n_i \diagup n \qquad \text{Eqn. A2}$$

where n_i is the number of moles of species i and $n = \sum n_i$ is the total number of moles of all gases. It follows that

$$\sum X_i = 1 \qquad \text{Eqn. A3}$$

and, if we assume that dry air contains, at most, oxygen, carbon dioxide, carbon monoxide and nitrogen, then

$$X_{O2} + X_{CO2} + X_{CO} + X_{N2} = 1 \qquad \text{Eqn. A4}$$

for both the supply and the exhaust. Since nitrogen is non-reactive (under normal fire conditions), the number of moles of nitrogen is conserved and

$$\dot{n}^1 X^1_{N2} = \dot{n}^0 X^0_{N2} \qquad \text{Eqn. A5a}$$

or

$$\dot{n}^1 = \dot{n}^0 (X^0_{N2} \diagup X^1_{N2}) \qquad \text{Eqn. A5b}$$

where $\dot{n}^0$ and $\dot{n}^1$ are the total molar flow rates for the supply and exhaust, respectively. Solving for X_{N2} in Equation A4 and substituting into Equation A5, we get

$$\dot{n}^1 = \dot{n}^0 [(1 - X^0_{O2} + X^0_{CO2}) \diagup (1 - X^1_{O2} + X^1_{CO2} + X^1_{CO})] \qquad \text{Eqn. A6}$$

where we have assumed that there is no carbon monoxide in the supply air (that is, X^0_{CO} is zero).

We can rewrite Equation A1, in terms of the mole fractions and total molar flows, as

$$\Phi = (X^0_{O2}\,\dot{n}^0 - X^1_{O2}\,\dot{n}^1) \,/\, X^0_{O2}\,\dot{n}^0 \qquad \text{Eqn. A7}$$

and, replacing $\dot{n}^1$ with Equation A6, we get

$$\Phi = (X^0_{O2} - X^1_{O2}) \,/\, (X^0_{O2})\,[(1 - X^0_{O2} + X^0_{CO2}) \,/\, (1 - X^1_{O2} + X^1_{CO2} + X^1_{CO})] \qquad \text{Eqn. A8}$$

This can be expanded and rearranged to give

$$\Phi = X^0_{O2}\,(1 - X^1_{CO2} - X^1_{CO}) - X^1_{O2}\,(1 - X^0_{CO2}) \,/\, X^0_{O2}(1 - X^1_{O2} - X^1_{CO} - X^1_{CO2}) \qquad \text{Eqn. A9}$$

which was Equation 2 in section 3.1.

If we assume that the gases may be treated as ideal, then

$$n_i = PV_i \,/\, RT \qquad \text{Eqn. A10}$$

where n_i is the number of moles of species i, V_i is the volume of the same species, P and T are the system pressure and temperature, respectively, and R is the universal gas constant. Therefore, if the supply and exhaust volume flows have been corrected to the same pressure and temperature, we may use volume fractions instead of mole fractions in our calculations. Experimentally, this is convenient because gas analyzers normally provide outputs directly in volume fraction units.

1.2 The Heat Release Rate

In this section, we develop heat release rate equations for various combustion conditions. It is assumed that the fuels involved are hydrocarbons (*i.e.*, there are no heteroatoms) and that the fuel is completely burned, so that there are no residual hydrocarbons in the exhaust stream. Thus, the combustion products will be a mixture of carbon dioxide, carbon monoxide and water vapor

Under these assumptions, we may write a generic combustion reaction as

$$n_F\,F + n_{O2}\,O_2 = n_{CO2}\,CO_2 + n_{CO}\,CO + n_{H2O}\,H_2O \qquad \text{Rxn. A1}$$

where F is a hydrocarbon fuel of unspecified molecular composition.

1.2.1 Complete oxidation

The simplest assumption is that we have complete oxidation so that all of the carbon in the fuel is

converted into carbon dioxide and there is no carbon monoxide. For these conditions, Reaction A1 becomes

$$n_F F + n_{O2} O_2 = n_{CO2} CO_2 + n_{H2O} H_2O \qquad \text{Rxn. A2}$$

for which the net heat liberated per mass of oxygen, H_f, is approximately 13.1 MJ/kg oxygen for most hydrocarbon fuels [5]. Thus, the heat release rate for complete fuel combustion is given by

$$Q_f = H_f M_{O2} (\dot{n}^0_{O2} - \dot{n}^1_{O2}) \qquad \text{Eqn. A11}$$

where Q is HRR in MW, M_{O2} is the molecular weight of oxygen (32 gm/mol), H_f is again the heat release per mass of oxygen consumed by combustion of the fuel, $\dot{n}^0_{O2}$ is the molar supply rate of oxygen and $\dot{n}^1_{O2}$ is the molar exhaust rate for oxygen.

From the definition of the oxygen consumption factor (Equation A1), we have

$$Q_f = H_f \Phi M_{O2} \dot{n}^0_{O2} \qquad \text{Eqn. A12}$$

but $\dot{n}^0_{O2}$ is related to the total number of moles of gas, $\dot{n}^0$ via the mole fraction. Therefore,

$$Q_f = H_f \Phi M_{O2} \dot{n}^0 X^0_{O2} \qquad \text{Eqn. A13}$$

1.2.2 Partial oxidation

For the oxidation of carbon monoxide, we have

$$2 CO + O_2 = 2 CO_2 \qquad \text{Rxn. A3}$$

for which H_{CO}, the heat of combustion per mass of oxygen, is 17.6 MJ/kg [7].

Conceptually, we can consider that the fuel was completely oxidized, as in Reaction A2, and that a portion of the carbon dioxide product then reacts to produce carbon monoxide and oxygen, using the reverse of the reaction given in Reaction A3. The net reaction is then the sum of two reactions:

$$n_F F + n_{O2} O_2 = n_{CO2} CO_2 + n_{H2O} H_2O \qquad \text{Rxn. A4a}$$
$$+ (2 \Delta n_{CO2} CO_2 = 2 \Delta n_{CO2} CO + \Delta n_{CO2} O_2) \qquad \text{Rxn. A4b}$$

which can be rearranged to

$$n_F F + (n_{O2} - \Delta n_{CO2}) O_2 = (n_{CO2} - 2\Delta n_{CO2}) CO_2 + n_{H2O} H_2O + 2 \Delta n_{CO2} CO \qquad \text{Rxn. A5}$$

The net heat release for the 2 Δn_{CO2} moles of carbon dioxide that undergo the back reaction is then defined as

$$\Delta \equiv H_f - H_{CO} \qquad \text{Eqn. A14}$$

From Equation A1, we have

$$\dot{n}^1_{O2} = \dot{n}^0_{O2} (1 - \Phi) \qquad \text{Eqn. A15}$$

which is a measure of the residual oxygen after combustion. Casting this in terms of the total molar flow rates in the supply and exhaust, we get

$$\dot{n}^1 X^1_{O2} = \dot{n}^0 X^0_{O2} (1 - \Phi) \qquad \text{Eqn. A16a}$$

or

$$\dot{n}^1 = \dot{n}^0 (1 - \Phi) (X^0_{O2} / X^1_{O2}) \qquad \text{Eqn. A16b}$$

and the molar flow rate of carbon monoxide in the exhaust stream is then

$$\dot{n}^1_{CO} = \dot{n}^0 (1 - \Phi) (X^0_{O2} / X^1_{O2}) X^1_{CO} \qquad \text{Eqn. A17}$$

From the stoichiometry of Reaction A3, we know that the molar reaction rate of oxygen is half that of carbon monoxide, so it follows that

$$\dot{n}^{CO}_{O2} = \dot{n}^0 [(1 - \Phi) / 2] (X^0_{O2} / X^1_{O2}) X^1_{CO} \qquad \text{Eqn. A18}$$

where $\dot{n}^{CO}_{O2}$ is the oxygen production rate from the conversion of carbon dioxide to carbon monoxide plus oxygen. The heat production due to the carbon monoxide reaction is then

$$Q_{co} = \Delta [(1 - \Phi) / 2] (X^1_{CO} / X^1_{O2}) M_{O2} \dot{n}^0 X^0_{O2} \qquad \text{Eqn. A19}$$

Combining Equations A15 and A21 to get the total heat production, we have

$$Q = \left[H_f \Phi - (H_{CO} - H_f) [(1 - \Phi) / 2] (X^1_{CO} / X^1_{O2}) \right] M_{O2} \dot{n}^0 X^0_{O2} \qquad \text{Eqn. A20}$$

where we have substituted for Δ and reversed the sign of that term to be consistent with common usage.

1.2.3 Wet gas

In the above, we have assumed all of the X_i terms are dry air values. This is convenient, because air is normally filtered and dried upstream of the gas analyzers to prevent clogging or corrosion of the sample lines and interference with the sensor elements. However, we must now correct for

the fact that water vapor was actually present in the system.

Consider a system composed of n moles total, of which n_{H2O} are water vapor. The number of moles of dry air is then

$$n_{dry} = n - n_{H2O} \qquad \text{Eqn. A21}$$

and the mole fractions may be written as

$$X_i = n_i \,/\, n \qquad \text{Eqn. A22}$$

or

$$X_{i,dry} = n_i \,/\, (n - n_{H2O}) \qquad \text{Eqn. A23}$$

for wet and dry measurements, respectively. Thus, we can relate the two measurements by

$$X_i \,/\, X_{i,dry} = 1 - n_{H2O} \,/\, n \qquad \text{Eqn. A24}$$

which, in terms of the mole fraction of water vapor[6], becomes

$$X_i \,/\, X_{i,dry} = 1 - X_{H2O} \qquad \text{Eqn. A25}$$

Mole fractions enter into Equation A20 in two places: the ratio (X^1_{CO}/X^1_{O2}) and the term X^0_{O2}. From Equation A25, it follows that mole fraction ratio has the same value regardless of whether it is expressed in wet or dry measurements. Thus, the only change that needs to be made to Equation A20 is to correct the X^0_{O2} term to a wet basis, giving

$$Q = \left[H_f \,\Phi - (H_{CO} - H_f)\,[(1 - \Phi) \,/\, 2]\,(X^1_{CO}/X^1_{O2})\right] M_{O2}\, \dot{n}^0\, (1 - X_{H2O})\, X^0_{O2} \qquad \text{Eqn. A26}$$

1.2.4 Final Equation

Since the measurements are made in the exhaust stack, it is conventional to recast Equation A26 in terms of the exhaust molar flow rate, $\dot{n}^1$. Consider that the supply stream is composed of two components:

$$\dot{n}^0 = \dot{n}_{unreact} + \dot{n}_{deplete} \qquad \text{Eqn. A27}$$

where $\dot{n}_{unreact}$ is the gas that passed through the system unreacted and $\dot{n}_{deplete}$ is that which has completely reacted (is totally depleted of oxygen). From Equation A1, we see that Φ represents the depleted fraction and, therefore, $(1 - \Phi)$ represents the unreacted fraction.

After combustion, the lost oxygen has been more than replaced by combustion products,

[6] Experimentally, X_{H2O} is usually calculated from the measured relative humidity and temperature, rather than being directly measured, because water vapor sensors tend to be unreliable under test conditions.

resulting in an increase in the total number of moles of gas. This leads to an expansions of the gas volume (at constant temperature and pressure). The expansion factor, α, is defined as the ratio of moles of combustion products to moles of depleted air

$$\alpha \equiv \dot{n}_{prod} \diagup \dot{n}_{deplete} \qquad \text{Eqn. A28}$$

and we note that it is nearly constant (approximately 1.10) for typical fires [7]. Thus, the exhaust stream may be represented as the sum of the unreacted fraction plus the reacted fraction corrected for the increased number of moles of gas

$$\dot{n}^1 = \dot{n}^0 (1 - \Phi) + \alpha \dot{n}^0 \Phi \qquad \text{Eqn. A29}$$

With a minor rearrangement, this becomes

$$\dot{n}^0 = \dot{n}^1 \diagup [(1 + \Phi (\alpha - 1)] \qquad \text{Eqn. A30}$$

and the HRR is then

$$Q = \left[H_f \Phi - (H_{CO} - H_f) [(1 - \Phi) \diagup 2] (X^1_{CO}/X^1_{O2})\right] M_{O2} * \left(\dot{n}^1 \diagup [(1 + \Phi (\alpha - 1)]\right) (1- X_{H2O}) X^0_{O2} \qquad \text{Eqn. A31}$$

By convention, the mass flow rate is usually used instead of the molar flow rate so that we have

$$Q = \left[H_f \Phi - (H_{CO} - H_f) [(1 - \Phi) \diagup 2] (X^1_{CO}/X^1_{O2})\right] M_{O2} \diagup M_e * \left(\dot{m}^1 \diagup [(1 + \Phi (\alpha - 1)]\right) (1- X_{H2O}) X^0_{O2} \qquad \text{Eqn. A32}$$

where M_e, the effective molecular weight of the exhaust gas, is usually approximated by the molecular weight of air.

Consider the extreme case of pure carbon burned to pure carbon monoxide. The effective molecular weight of the supply gas is

$$M_s = X^0_{N2} M_{N2} + X^0_{O2} M_{O2} = 28.8 \text{ gm/mol} \qquad \text{Eqn. A33}$$

For the exhaust gas, the number of moles of nitrogen remains the same as in the supply and the number of moles of carbon dioxide is twice the number of moles of oxygen in the supply. Consequently, the effective exhaust molecular weight is

$$M_e = X^0_{N2} M_{N2} + 2 X^0_{O2} M_{CO} = 28.0 \text{ gm/mol} \qquad \text{Eqn. A34}$$

so there is an error of less than 3% if the supply side value is used.

Making the substitution for M_e, the final HRR equation (Equation 3 in section 3.1) is then

$$Q = \left[H_f \Phi - (H_{CO} - H_f)\,[(1 - \Phi) / 2]\,(X^1_{CO}/X^1_{O2})\right] M_{O2} / M_{air} * \left(\dot{m}^1 / [(1 + \Phi\,(\alpha - 1)]\right)\,(1 - X^0_{H2O})\,X^0_{O2} \qquad \text{Eqn. A35}$$